Int. J. Heat Mass Transfer. Vol. 35, No. 12, pp. 3313–3321, 1992
Printed in Great Britain

0017–9310/92 $5.00 + 0.00

Thermal radiation modeling in multilayer thin film structures

PETER Y. WONG, CHRISTOPHER K. HESS and IOANNIS N. MIAOULIS†
Thermal Analysis of Materials Processing Laboratory, Mechanical Engineering Department, Tufts University, Medford, MA 02155, U.S.A.

(*Received* 15 *October* 1991 *and in final form* 31 *January* 1992)

Abstract—A general technique is developed to account for the microscale heat transfer effects involved with the interaction of thermal radiation and multilayer thin films. In particular, the microscale radiation effects involved with both the emission from the multilayer structure and the reflection of incident radiation are described in detail. Considerable optical interference within the structure occurs when the film thicknesses are on the same order of magnitude as the wavelengths of the incident or emitted radiation; therefore, the net surface reflectivity and emission from the film structure are altered by slight changes in film thickness. Consequently, during high temperature thermal processing of micron thickness films, the resultant temperature profiles and the quality of the processed structure will be affected. The reflectivities and emissivities are calculated numerically using the matrix method for several different layering structures subject to thermal radiation. For the special case of equal optical film thicknesses, cross-correlation peaks are identified; these layering schemes are very sensitive to small film thickness changes. Maximum temperatures attained during thermal processing are calculated for several specific film structures to illustrate the significance of these effects.

1. INTRODUCTION

THERMAL treatment of multilayer thin film (~ 1 μm) structures with a heat source emitting in the thermal radiation spectrum range (0.2 μm $< \lambda <$ 8.0 μm) is a common procedure in numerous electronic and optical material processes. There is a variety of heat sources currently used, such as graphite strip heaters, halogen lamp heaters, lasers, and flash heaters. Temperature prediction and control during such processes is critical since thermal gradients established during processing are responsible for material defects. The small film thickness and the high temperatures involved make it difficult to determine temperature distributions experimentally. Thus costly trial-and-error techniques are typically used for parameter optimization. The need for temperature prediction in such processes and the difficulties associated with experimental monitoring has led most investigators to simulate these processes numerically. Several investigators have already proposed models to account for the critical heat transfer parameters involved. However, most of these studies neglect the microscale optical effects of multilayer thin films during thermal processing.

There is a considerable amount of optical interference within the multilayer structure when the film thicknesses are on the same order of magnitude as the incident radiation [1]. The net surface reflectivity and absorption can change significantly with a change in any of the film thicknesses. The resultant temperature profiles and quality of the film are therefore affected by these changes in optical properties.

The majority of the previous studies on the optical effects of thin films focus on a monochromatic radiation source. One of the first studies conducted was that of Tamura *et al.* [2], in which the behavior of a silicon substrate capped with a thin SiO_2 film during laser annealing was investigated. The results indicated a periodic relationship between transmissivity and film thickness, which closely agreed with experiments. A numerical model employing the matrix method [3, 4] was developed by Colinge and Wiele [5] to determine the laser power absorbed in a silicon-on-insulator (SOI) structure while taking into account the optical effects of the thin films. Several one-dimensional, two-dimensional, and semi-empirical models have been developed to determine the temperature profiles for laser processing. Grigoropoulos *et al.* [6] have developed a 3-D numerical model of a SiO_2/Si/SiO_2 film structure which includes melting by employing the enthalpy method.

The numerical model proposed by Wong *et al.* [1] involves the use of radiant heat source (graphite strip heater), which includes the full spectrum of wavelengths emitted from the strip heater, and determines the reflectivity along the length of the wafer. The model predicts the temperature distribution in the oxide capped SOI system for under-melting temperatures; however, the change in emissivity with film thickness was not considered. The model was modified to include melting and similar results were presented [7, 8]. A maximum reflectivity value that is very sensitive to thickness variation was observed at equal

† Author to whom all correspondence should be addressed.

NOMENCLATURE

a_{film} thermal diffusivity of the film
a_{sub} thermal diffusivity of the substrate
d_{film} thickness of the film
$e_{b\lambda}$ monochromatic emissive power
$F_{1-2}(\phi)$ radiation shape factor for a given angle
$F_{1-2}(x)$ radiation shape factor to a given point
k_{film} thermal conductivity of the film
n real part of index of refraction
$\mathbf{n}$ complex index of refraction
$q_{film}(x)$ radiative heat flux through the film for a given point
T_{film} temperature of the film
T_{heater} temperature of the heater
T_{sub} temperature of the substrate
$W(\phi)$ weighting function.

Greek symbols
$\alpha(\lambda, \phi)$ absorptivity of the film structure for a given angle and wavelength
$\alpha_{point}(x)$ total absorptivity from a given point
$\varepsilon(\lambda, \phi)$ emissivity from the film structure for a given angle and wavelength
ε_{total} total hemispherical emissivity
θ time
κ extinction coefficient; imaginary part of index of refraction
λ wavelength of radiation
$\rho(\lambda, \phi)$ reflectivity from the surface of the film structure for a given angle and wavelength
$\rho_{angle}(\phi)$ total reflectivity from a given angle
$\rho_{point}(x)$ total reflectivity from a given point
σ Stefan–Boltzmann constant
$\tau(\lambda, \phi)$ transmissivity of film structure for a given angle and wavelength
ϕ angle of incidence at an interface
ϕ_{max} maximum angle from normal between point on film and heater
ϕ_{min} minimum angle from normal between point on film and heater.

oxide thicknesses; further investigation established that this phenomenon is due to a cross-correlation of the oxide reflectivity functions [9]. These studies present the effects of microscale radiation phenomena on the structure reflectivity, and determine the temperature distribution neglecting emissivity microscale effects. Results are focused on a specific structure (SOI), and cannot be used for general film modeling.

This paper presents a general technique for calculating the reflectivity and emissivity in any number of thin films during processing with a radiant heat source. Specific examples are used to illustrate the importance of these radiation effects. Arrangements of silicon and silicon oxide films were used as materials in most examples, so that the effects presented could be compared with previous studies. Reflectivity, emissivity and maximum temperature changes are presented as a function of film thickness for an optically thick substrate, and single thin film, two films, and three films on substrate. In order to isolate the radiative effects, heat losses by convection on the surface of the structure and phase change effects are not considered.

2. INTERACTION OF THERMAL RADIATION AND MULTILAYER STRUCTURES

The mechanics of radiation heat transfer between bodies is well understood. For heated bodies, the range of radiative energy distribution in the electromagnetic spectrum is usually limited to the thermal radiation spectrum, 10^{-4}–10^{-7} m. The relation of energy density of radiation to temperature and wavelength is described by Planck's radiation law.

The interaction between thermal radiation and solid objects is dependent on the complex index of refraction of the solid and the wavelength range of the radiation. The complex index of refraction, $\mathbf{n}$, consists of a real part, n, and an imaginary part, κ. The interaction of radiation and solids can be understood by observing the interaction of a single wavelength and the solid. In the two-dimensional case, plane waves incident to an interface will split up into reflected and transmitted waves. For multilayer structures there will be reflected and transmitted waves at each interface which will interfere with each other. The net surface reflectivity can be found by summing up the waves exiting the structure and re-entering the initial medium. Similarly, the net transmission can be found by summing up the waves passing through the structure. Resolving the reflectance, $\rho(\lambda, \phi)$, and transmittance, $\tau(\lambda, \phi)$, for a single wavelength and a single angle of incidence involves solving Maxwell's equations in each medium and applying the appropriate boundary conditions. This is done by using the matrix method [3].

2.1. *Technique to determine reflectivity for incident thermal radiation*

The total reflectance of thermal radiation at a single angle of incidence, $\rho_{angle}(\phi)$, is the sum of the waves leaving the structure and re-entering the initial medium, where the amount of energy carried in a particular wavelength is dependent on Plank's distribution. The total reflectance can therefore be evaluated by integrating over the thermal radiation spectrum,

$$\rho_{\text{angle}}(\phi) = \frac{\int_{10^{-7}}^{10^{-4}} \rho(\lambda, \phi)\varepsilon_{\text{heater}} e_{b\lambda}(T_{\text{heater}})\,d\lambda}{\sigma T_{\text{heater}}^4} \quad (1)$$

where $e_{b\lambda}$ is the monochromatic emissive power of a blackbody emitter [W m^{-3}] and the total reflected energy has been normalized to the Stefan–Boltzmann law. The sensitivity of reflectivity to film thickness change is strongest when the film thickness is on the same order of magnitude as the wavelength. In the thermal radiation spectrum, the size of the wavelength varies by three orders of magnitude. However, the largest portion of the energy is carried by a smaller range of wavelengths. Any change in optical parameters for these wavelengths results in the largest overall change in total optical property. The significant range of wavelengths can be approximated to center around $\lambda_{\max}$, which depends on the temperature of the emitting heat source, derived by Wien's displacement law.

For cases where the energy is incident upon the surface at a range of angles of incidence, the total reflected energy from a point on the structure is the sum of the reflected energy at all angles leaving the surface. For the case of a finite size heater, the range of angles that are incident to a point on the structure is dependent on the geometry of the heat source. The distribution of incident energy per angle can be expressed as a weighting of the shape factor for that particular angle to the total shape factor between the point in question and the heat source

$$W(\phi) = \frac{F_{1-2}(\phi)}{\int_{\phi_{\min}}^{\phi_{\max}} F_{1-2}(\phi)\,d\phi} \quad (2)$$

where $F_{1-2}(\phi)$ is the shape factor, the ratio of incident energy at a point to the total energy, and $\phi_{\max}$ and $\phi_{\min}$ are the maximum and minimum viewing angles respectively. In our analysis, the Hottel cross string method is used to determine these shape factors [10]. The total reflectance to a point, $\rho_{\text{point}}(x)$, from several angles and several wavelengths can then be calculated as

$$\rho_{\text{point}}(x) = \int_{\phi_{\min}}^{\phi_{\max}} \rho_{\text{angle}}(\phi) W(\phi)\,d\phi. \quad (3)$$

2.2. *Technique for determining the total hemispherical emissivity*

The multilayer structure emits thermal radiation, following Planck's radiation law, over a hemispherical volume. There will be interference within the structure due to internal reflections and refractions that affect the total hemispherical emissivity. For any semi-transparent multilayer structure the absorptivity is given by

$$\alpha(\lambda, \phi) = 1 - \rho(\lambda, \phi) - \tau(\lambda, \phi). \quad (4)$$

From Kirchoff's law, the spectral-directional emissivities are equal to the respective absorptivities in equation (4). The total surface emissivity may be found by assuming an isothermal structure and therefore is assumed constant along the surface of the structure. The total hemispherical emissivities can be determined by integrating first over all angles and then with respect to wavelength using Planck's radiation law,

$$\varepsilon_{\text{total}} = \frac{\int_{10^{-7}}^{10^{-4}} \int_0^{\pi} (1 - \rho(\lambda, \phi) - \tau(\lambda, \phi)) e_{b\lambda}(T_{\text{structure}})\,d\phi\,d\lambda}{(\pi)(\sigma T_{\text{structure}}^4)}. \quad (5)$$

However, for the special case of optically thick materials where the thermal radiation is absorbed within a few microns from the surface, $\tau(\lambda, \phi) = 0$.

3. MODELING OF THERMAL PROCESS

For high temperature thermal processing of multilayer thin film structures, the film thicknesses which produce the most sensitive radiative property changes are of the order of microns. Specifically for graphite strip heaters at $\sim 2000°C$, $\lambda_{\max}$ is ~ 1.7 μm and the important wavelengths are in the range between 0.2 μm and 8.0 μm. In order to optimize the thermal process, it is important to obtain the temperature distribution within the structure. Heat transfer analyses for these thin films have typically neglected the microscale heat conduction and radiation effects. For thin films the temperature gradient across the thickness of the film can be ignored and therefore the conduction effects within the thin films are negligible in this direction [11].

In order to illustrate the microscale radiation effects on the temperature distribution, the heating of a multilayer structure subjected to thermal radiation from a graphite strip heater with a 3 mm × 1 mm cross section that is considered to be 2 mm above the surface of the structure was modeled. As an example, this model simulates the graphite strip heating of a silicon substrate with stacked thin films. A schematic of such a process is shown in Fig. 1.

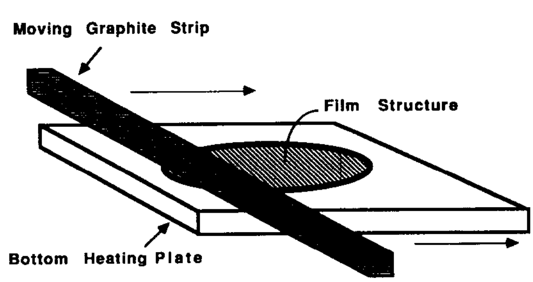

FIG. 1. Schematic of the process.

The governing differential equation of heat transfer in a thin film is given by

$$\frac{\partial^2 T_{\text{film}}}{\partial x^2}+\frac{\partial^2 T_{\text{film}}}{\partial y^2}+\frac{q_{\text{film}}(x)}{k_{\text{film}}d_{\text{film}}}=\frac{1}{a_{\text{film}}}\frac{\partial T_{\text{film}}}{\partial \theta} \quad (6)$$

where the heat flux q_{film} can be approximated as

$$q_{\text{film}}(x)=\alpha_{\text{point}}(x)F_{1-2}(x)\sigma T_{\text{heater}}^4-\varepsilon_{\text{total}}\sigma T_{\text{film}}^4 \quad (7)$$

where T_{film} is the temperature within the film, k_{film} is the thermal conductivity of the film, d_{film} is the thickness of the film, $\alpha_{\text{point}}(x)$ is the absorptivity distribution across the thin film surface, $F_{1-2}(x)$ is the radiation shape factor from the point in question to the strip heater, σ is the Stefan–Boltzmann constant, T_{heater} is the temperature of the radiant heater, $\varepsilon_{\text{total}}$ is the emissivity from the surface, and a_{film} is the thermal diffusivity of the film. The substrate is considered optically thick; thus, $\alpha_{\text{point}}(x)=1-\rho_{\text{point}}(x)$. For the substrate the heat transfer in two dimensions is represented by

$$\frac{\partial^2 T_{\text{sub}}}{\partial x^2}+\frac{\partial^2 T_{\text{sub}}}{\partial y^2}=\frac{1}{a_{\text{sub}}}\frac{\partial T_{\text{sub}}}{\partial \theta}. \quad (8)$$

The domain was discretized to model a 60 mm diameter × 0.4 mm thick wafer. The strip is considered stationary at the center of the wafer to take advantage of this configuration's symmetry. Thus only half the wafer is modeled. An uneven grid is used to optimize the computational time needed to solve the matrix. The grid is finer in the area beneath the strip to account for the steeper temperature gradients. The horizontal grid spacing is as small as 20 μm underneath the strip and as large as 500 μm near the edge of the wafer. The grid spacing in the vertical direction is 100 μm throughout the wafer. However, the control volume of the surface nodes only extends down 1 μm from the surface. This allows the thin film at the surface to be accurately characterized.

For these studies the substrate thermal properties are assumed to be silicon's. The thermal conductivity of silicon is assumed to have a constant value of 0.2 W m^{-1} K^{-1}, the value of the temperature dependent thermal conductivity at a temperature near its melt point, 1412°C. This gives reasonably good results compared to a temperature dependent solution [11]. The values of specific heat and density are 0.98 W kg^{-1} °C^{-1} and 2.3 g cm^{-3} respectively. Thermal properties in the substrate affect the temperature greatly, while the film's thermal properties affect the results only slightly because of its small size. The boundary condition on the bottom of the substrate is a radiative exchange with a bottom susceptor heater. The edges of the film and substrate are assumed to be insulated for these studies. The initial temperature of the entire wafer is 1000°C.

The addition of thin films to the surface affects only the radiative input and resultant reflectivity and emissivity profiles. The conduction effects remain the same. The analysis focuses on the changes in thermal radiation reflectivity and emissivity with changes in the film optical properties and thickness.

4. ANALYSIS

The analysis, using the technique and model described in the previous sections, focuses on identifying thin film effects that result from optical interference between the films and the thermal radiation spectrum. For these studies, various silicon and silicon oxide structures were used for illustration. Constant indices of refraction are used here to illustrate the technique presented. The complex index of refraction of silicon is $3.5-0.05i$, while that of silicon oxide is $1.5-0.0i$. Several multilayer structure arrangements are examined (Fig. 2).

4.1. *Single optically thick film (substrate)*

First an unlayered thick substrate, $\mathbf{n}=n-0.05i$, was investigated, where the index of refraction, n, was varied (Fig. 2a). The reflectivity and emissivity do not vary with wavelength or strip temperature unless there are considerable reflections from the bottom interface of the substrate. The extinction coefficient, κ, dictates when the optical thickness of the substrate becomes important to consider. If the substrate is considered optically thick (i.e. all the energy is absorbed within several microns), then the reflectivity becomes dependent only on the optical properties of the material and the angle of incidence.

Increasing the real index of refraction of the substrate, the reflectivity and emissivity of the surface change dramatically. As expected, reflectivity was found to increase (Fig. 3a) and emissivity decrease (Fig. 3b) as a function of index of refraction.

4.2. *One film on substrate*

The next structure considered consists of a 1 μm thick film ($\mathbf{n}=1.5-0.0i$) on a substrate ($\mathbf{n}=3.5-0.05i$) (Fig. 2b). As the temperature of the strip changes, the critical wavelengths which carry the most energy change according to Plank's radiation law. The reflectivity from the structure will change with the shifting of the critical wavelengths. However, the

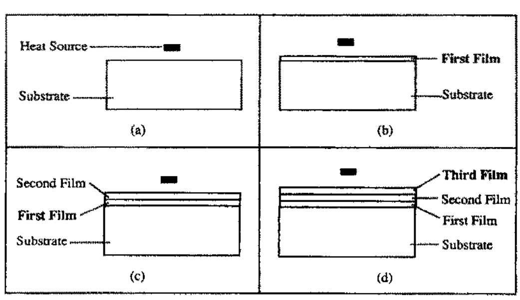

FIG. 2. Schematic of structures heated by a black body heater: (a) substrate only, (b) one film on substrate, (c) two films on substrate, (d) three films on substrate.

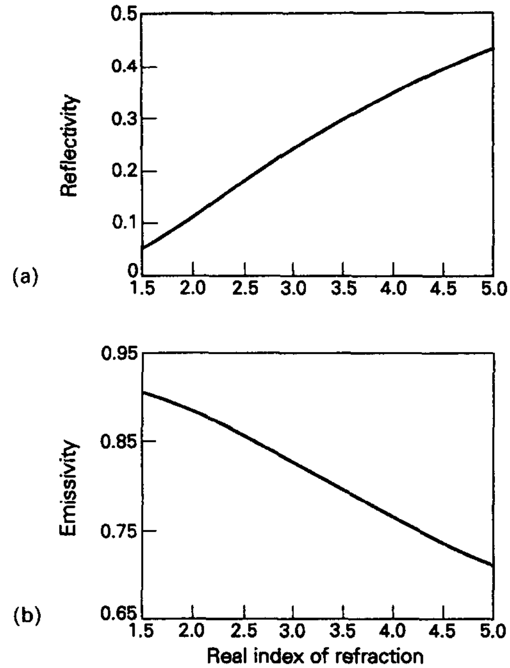

FIG. 3 (a) Effect of varying real index of refraction of substrate on the reflectivity directly beneath the strip heater. (b) Effect of varying real index of refraction of substrate on the total hemispherical emissivity.

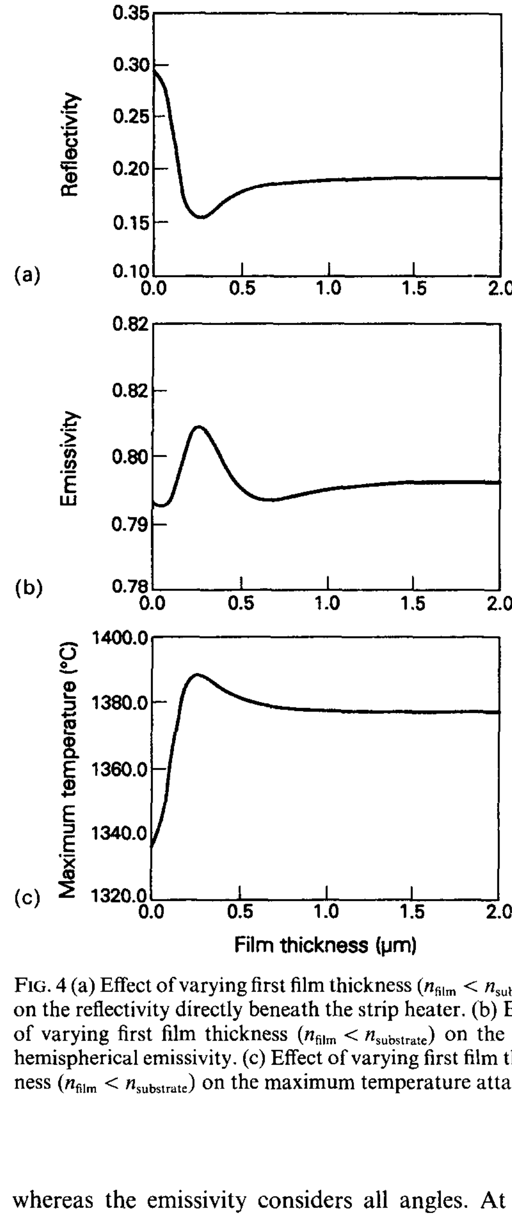

FIG. 4 (a) Effect of varying first film thickness ($n_{\text{film}} < n_{\text{substrate}}$) on the reflectivity directly beneath the strip heater. (b) Effect of varying first film thickness ($n_{\text{film}} < n_{\text{substrate}}$) on the total hemispherical emissivity. (c) Effect of varying first film thickness ($n_{\text{film}} < n_{\text{substrate}}$) on the maximum temperature attained.

effect is very small ($\sim 1\%$) for typical processing temperatures.

In this study, the film thickness was varied from 0.0 to 2.0 μm in steps of 0.05 μm for a strip heater temperature of 2050°C. The reflectivity directly under the strip as a function of film thickness is shown in Fig. 4(a). The reflectivity initially drops and then rises to a steady value of ~ 0.192. The drop is attributed to the thickness of the film which is smaller than the wavelengths of the relevant radiation spectrum range. The reflections from the second interface for all wavelengths are in phase with the reflection from the first interface for near zero film thicknesses. As the film thickness increases, the larger wavelengths notice little change while the smaller wavelengths begin to shift out of phase. The shifting out of phase of the reflected waves translate to a decrease in total reflectivity. This effect is observed for thicknesses up to 0.25 μm. As the thickness continues to increase, the reflectivity rises to a steady value as constructive and destructive interference cancel out.

The trend for emissivity is generally the inverse of reflectivity. However, a slight decrease in emissivity is observed at a thickness of 0.05 μm shown in Fig. 4(b). For thickness larger than 0.05 μm, emissivity rises then drops off to a constant value of ~ 0.796. This slight decrease at 0.05 μm can be understood by considering the spectral-directional emissivity in terms of reflectivity. Total reflectivity of a point only involves the range of angles radiated from the strip to the point, whereas the emissivity considers all angles. At this small thickness, the wavelengths that are larger than the film thickness contribute little to the reflectivity change. The inclusion of the shorter wavelengths at larger angles are shifting into phase to create a decrease in emissivity. The absolute values of emissivity are slightly higher than experimental values obtained for silicon because constant optical values are used in the calculation.

For a given structure, generally as reflectivity increases, emissivity decreases. Thus, reflectivity and emissivity have a cancelling effect on the heat radiated to and from the structure. In this single film structure however, the importance of reflectivity due to a change in film thickness dominates the determination of the maximum temperature attained under the strip. This occurs because the heat source is over 600°C higher than the wafer surface temperature and therefore the reflectivity plays a greater role in the radiation heat transfer interaction with the wafer. As the film thickness increases from zero thickness, the maximum temperature rises because of the strong influence of the decrease in reflectivity (Fig. 4c). There is an initial change of 50°C in maximum temperature as the film thickness increases from zero to 0.30 μm. As both reflectivity and emissivity approach constant values at larger film thicknesses, the temperature drops slightly and reaches a constant value of ~1376°C. In terms of film structure processing, it is evident that the thickness of the capping film is important to consider in a heat transfer analysis.

In the previous study, the index of refraction of the film was lower than the index of the substrate. When the index of the film is higher than the substrate, $\mathbf{n} = 4.5-0.0i$, nearly opposite effects occur with increasing thickness. The reflectivity will initially increase rather than decrease (Fig. 5a). The reflection off the second interface is initially out of phase with the reflection from the first interface. An increase in film thickness will bring the two reflections into phase up to a point and then the resultant reflectivity will approach a steady value. Emissivity decreases with increasing thickness, it then increases slightly, and then settles to a steady value (Fig. 5b). The decrease at small film thicknesses observed above does not occur because the change in the film's real index of refraction decreases the angles of radiation in the film and eliminates the effects of larger angles.

4.3. *Two films on substrate*

This study focused on the effects of adding a second film ($\mathbf{n} = 3.5-0.05i$) on top of the previous film ($\mathbf{n} = 1.5-0.0i$) on substrate ($\mathbf{n} = 3.5-0.05i$). The second film thickness is held constant at 1.0 μm as the first film thickness is varied from 0.0 μm to 2.0 μm (Fig. 2c). The results shown in Fig. 6(a) depict a different effect than a single film added to the surface. When the thickness of the first film is very small, the energy that would otherwise be transmitted into the substrate is partially reflected by the film. The reflection from the second interface is out of phase with the third interface reflection. As the thickness increases from zero, the reflections come into phase with each other, and the reflectivity increases initially for small thicknesses up to 0.3 μm. As the thickness continues to increase, the reflectivity falls to a steady value of ~0.365. The trends of emissivity are again the inverse of reflectivity. Emissivity initially decreases and then increases to a steady value of ~0.703 as shown in Fig. 6(b).

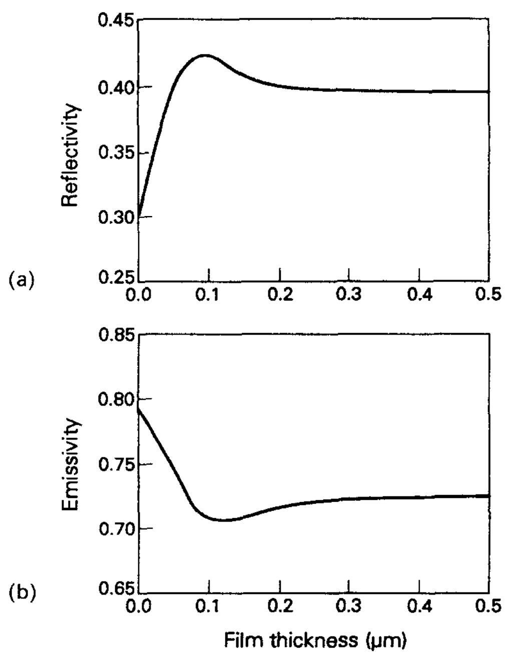

FIG. 5 (a) Effect of varying first film thickness ($n_{\mathrm{film}} > n_{\mathrm{substrate}}$) on the reflectivity directly beneath the strip heater. (b) Effect of varying first film thickness ($n_{\mathrm{film}} > n_{\mathrm{substrate}}$) on the total hemispherical emissivity.

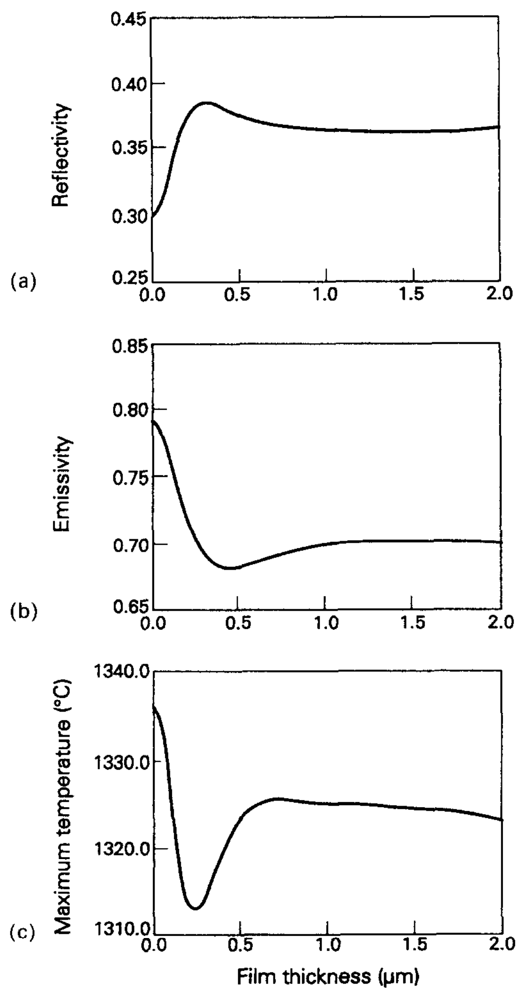

FIG. 6 (a) Effect of varying first film thickness ($n_{\mathrm{film}} < n_{\mathrm{substrate}}$) on the reflectivity directly beneath the strip heater; for two films on substrate. (b) Effect of varying first film thickness ($n_{\mathrm{film}} < n_{\mathrm{substrate}}$) on the total hemispherical emissivity; for two films on substrate. (c) Effect of varying first film thickness ($n_{\mathrm{film}} < n_{\mathrm{substrate}}$) on the maximum temperature attained; for two films on substrate.

The maximum temperature is again strongly dependent on the reflectivity values (Fig. 6c). Although emissivity decreases by ~ 0.11 to its minimum, as film thickness increases from zero, and reflectivity increases by only ~ 0.08, the temperature decrease in this region shows the significance of reflectivity in the final temperature profiles. The temperature rises at 0.3 μm and settles to a constant value of ~ 1324°C. In fact, these two films on the substrate represent a silicon-on-insulator (SOI) structure commonly used in the electronics industry. The maximum temperature attained depends strongly on the silicon dioxide film thickness due to radiative property changes.

When the index of refraction of the first film is greater than the index of refraction of the substrate, the reflections off the second and third interfaces are still out of phase. The same trends occur for both reflectivity and emissivity (Figs. 7a and 7b), although smaller absolute changes are noticed.

The interference effects for small thicknesses are considerable and depend on the ratios of the indices of refraction between the film and the substrate. As the films further increase in thickness, the thermal conductive effects may become more important. For large thicknesses, the contribution of the optical effects may decrease since the waves attenuate over the thickness.

4.4. *Three films on substrate*

An interesting layering structure to analyze, in order to illustrate the effects of a three film structure, is the common SOI layering scheme with a capping SiO_2 film. The first film on a silicon substrate is an insulating silicon oxide film, the second film is silicon, and the third film is silicon oxide. The effect of varying the third film's thickness while the other two are kept constant have already been shown [1]. The film thickness was varied from 0.5 to 2.0 μm while the other films' thicknesses were held at 1.0 μm. The results indicated the same complex behavior of the optics within the multilayer structure. Above melting [7, 8] and below melting [1] temperatures were considered without considering the changes in emissivity. An interesting phenomenon occurred at equal oxide thickness layering schemes which is characterized by a maximum reflectivity and minimum temperature. Any slight change in either oxide thickness resulted in significant changes in reflectivity which could seriously alter the temperature profiles and the resultant quality of the film. This effect is due to a cross-correlation of the reflectivity functions from the two oxide films. The cross-correlation has been shown to occur for a large range of possible layering schemes [9].

With the inclusion of emissivity changes with film thicknesses, the study on varying the third film thickness was extended (Fig. 2d). The reflectivities and emissivities directly underneath the strip were calculated for varying capping film thickness from 0 to 5.0 μm (Figs. 8a and 8b). The very thin film effects that were identified with a single film on a substrate also apply in the multilayer case when the third film thickness is also very thin.

The cross-correlation effect occurs whenever there are at least two films with equal optical thickness, nd (Table 1). When the third film thickness is 1.0 μm, the first and third optical thicknesses are equal to 1.5 μm. When the third film thickness is 2.333 μm, the optical thickness is equal to the optical thickness of the second film, 3.5 μm. For a third film thickness of 3.333 μm the optical thickness is equal to the addition of the optical thicknesses of the first and second films. At these thicknesses, the reflectivity shows a peak. The cross-correlation effect is present with emissivity as well, but is not as well clearly defined. Between these points, emissivity is not held as constant, as with reflectivity, due to higher angle effects.

These cross-correlation phenomena can be seen in the maximum temperatures attained. At a third film thickness of 1.0 μm, the temperature drops to ~ 1358.2°C and then rises to a relatively constant value of ~ 1361.3°C and again drops at film thickness of 2.333 μm to ~ 1360.0°C (Fig. 8c). The temperature again levels off to ~ 1360.4°C and rises at thickness of 3.333 μm to ~ 1362.3°C. These changes appear to be minute; however, in terms of thermal processing of silicon wafers, these changes can drastically affect the quality of the resulting film. At very thin film thicknesses, the maximum temperature increases drastically for zero thickness to 0.2 μm and then decreases to the first cross-correlation point at 1.0 μm. Any

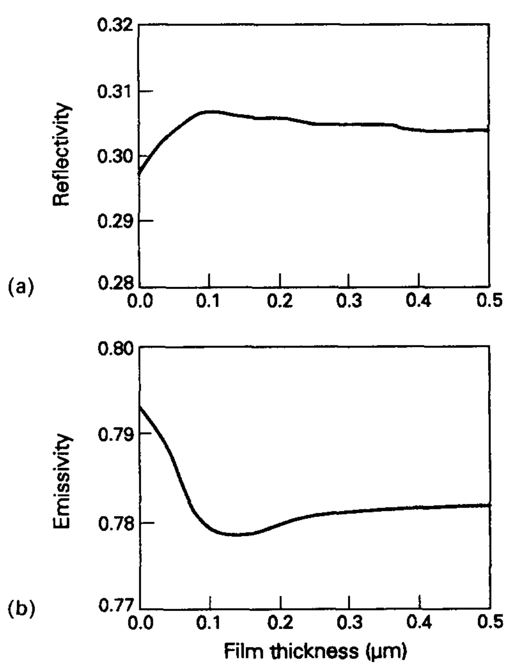

FIG. 7 (a) Effect of varying first film thickness ($n_{film} > n_{substrate}$) on the reflectivity directly beneath the strip heater; for two films on substrate. (b) Effect of varying first film thickness ($n_{film} > n_{substrate}$) on the total hemispherical emissivity; for two films on substrate.

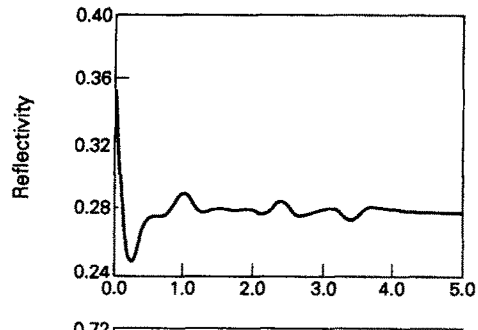

FIG. 8 (a) Effect of varying third film thickness ($n_{film} < n_{substrate}$) on the reflectivity directly beneath the strip heater; for three films on substrate. (b) Effect of varying third film thickness ($n_{film} < n_{substrate}$) on the total hemispherical emissivity; for three films on substrate. (c) Effect of varying third film thickness ($n_{film} < n_{substrate}$) on the maximum temperature attained; for three films on substrate.

materials process using this particular layering scheme should be designed taking into account this phenomenon in order to carefully monitor the temperature distributions in the wafers.

5. CONCLUSIONS

A general technique was developed to determine the radiative properties of a multilayer structure interacting with thermal radiation (0.2 μm $< \lambda <$ 8.0 μm). The microscale radiation effects in multilayer thin films were considered in a heat transfer analysis for processing with a radiant heat source. A model was developed to couple the optical and heat conduction models for a thick substrate with stacked thin films. With this technique the resultant temperature, in particular the maximum temperature attained, can be determined for various film thicknesses and processing conditions.

The effects of varying film parameters were examined for four different cases: optically thick film (substrate), and one film, two films, and three films on the substrate. The effect of different optical properties for an unlayered substrate on the reflectivity and emissivity were analyzed. As the index of refraction increases the reflectivity increases and the emissivity decreases.

In the case of one or two films on the substrate, the reflectivity, emissivity and temperature profile dependency on film thickness was considerable for film thicknesses below $\sim$0.3 μm. For greater thicknesses, the properties and maximum temperatures stayed fairly constant.

The reflectivities and emissivities for a capped SOI structure were calculated for capping film thicknesses that varied from 0.0 to 5.0 μm. There is still a drastic change in radiation properties for initial increasing thickness. The cross-correlation effect [9] was observed at equal optical thicknesses. For other thicknesses, the reflectivities remained fairly constant with slight deviations. This effect could also be seen in changes in emissivity, although not as clearly. However, the results of these effects could be seen in the maximum temperatures attained under the strip heater. Temperature dips were observed at 1.0 μm and 2.333 μm and a temperature rise was seen at 3.333 μm.

In each structure, the reflectivity was found to be very important in the determination of the maximum temperatures. Emissivity values were found to be higher than experimentally determined values because constant optical properties were used instead of wavelength dependent optical properties, but the same trends were captured. However, such optical data is scarce at elevated temperatures.

Table 1. Physical and optical thicknesses of films; three films on substrate

Film	n	Physical thickness (μm)	Optical thickness (μm)
First	1.5	1.0	1.5
Second	3.5	1.0	3.5
Third	1.5	x	$1.5x$

Acknowledgements—The authors wish to acknowledge Professor Lloyd M. Trefethen and Professor Paul Zavracky for their advice during the course of this study. This research was supported by the National Science Foundation under grants MSM-8817949 and CTS-9157278.

REFERENCES

1. P. Y. Wong, I. N. Miaoulis and P. Zavracky, Microscale heat transfer phenomena in multilayer thin film processing with a radiant heat source, *Proc. Symp. on Microstructures, Sensors, and Actuators*, Vol. 19, pp. 175–187. ASME Dynamic Systems and Control Division, New York (1990).

2. H. Tamura, M. Miyao and T. Tokuyama, Laser-annealing behavior of a phosphorus-implanted silicon substrate covered with a SiO_2 film, *J. Appl. Phys.* **50**(5), 3783–3784 (1979).
3. O. S. Heavens, *Optical Properties Of Thin Solid Films*, pp. 46–95. Buttersworth, Washington D.C. (1955).
4. Z. Knittl, *Optics of Thin Films*, pp. 240–282. Wiley Prague, Czechoslovakia, (1976).
5. J. P. Colinge and F. Van de Wiele, Laser light absorption in multilayers, *J. Appl. Phys.* **52**(7), 4769–4771 (1981).
6. C. P. Grigoropoulos, W. E. Dutcher, Jr. and A. F. Emery, Experimental and computational analysis of laser melting of thin silicon films, *J. Heat Transfer* **113**, 21–29 (1991).
7. P. Y. Wong, I. N. Miaoulis and P. Zavracky, Optical effects induced by the multilayer nature of SOI films during transient thermal processing with a radiant line heat source, *Proc. Symp. on Surface Chemistry and Beam Solid Interactions*, Vol. 201, pp. 445–450. Materials Research Society (1990).
8. P. Y. Wong and I. N. Miaoulis, Optical effects of multilayer thin-film structures during zone-melting recrystallization with an infrared heat source, *J. Appl. Phys.* **70**(12), 7594–7601 (1991).
9. P. Y. Wong, L. M. Trefethen and I. N. Miaoulis, Cross-correlation thermal radiation phenomena in multilayer thin-film processing, *Proc. Symp. on Microstructures, Sensors, and Actuators*, Vol. 32, pp. 349–359. ASME Dynamic Systems and Control Division, New York (1991).
10. H. C. Hottel and A. F. Sarofim, *Radiative Transfer*, pp. 31–33. McGraw-Hill, New York (1967).
11. I. N. Miaoulis, P. Y. Wong, J. D. Lipman and J. S. Im, Thermal modeling of zone-melting-recrystallization processing of silicon-on-insulator film structures, *J. Appl. Phys.* **69**, 7273–7282 (1991).